Int. J. Adv. Eng. Pure Sci. 2021, 33(1): 64-72
DOI: 10.7240/jeps.717399

RESEARCH ARTICLE / ARAŞTIRMA MAKALESİ

Investigation of Electronic Properties of SbSeI Under High Pressure by First Principles Calculations

Yüksek Basınç Altında SbSeI'nin Elektronik Özelliklerin İlk Hesaplamalar İle İncelenmesi

Tahsin ÖZER[1]

[1]*Osmaniye Korkut Ata University Bahçe Vocational High School, Osmaniye, Turkey.*

Abstract
The structural parameters, electronic structure, and charge density distribution of SbSeI compound under hydrostatic pressure of 0-200 kBar were investigated for the first time. Quantum Espresso software (QE) was used for all calculations. Electronic band calculations have shown that SbSeI has direct / indirect forbidden band gap in the 0-200 kBar pressure range.
Keywords: SbSeI, Pressure, Electronic properties, Quantum Espresso.

Öz
SbSeI'nın yapısal parametreleri, elektronik yapısı ve yük yoğunluğu dağılımı 0-200 kBar hidro statik basınç altında ilk kez araştırılmıştır. Tüm hesaplamalarda Quantum Espresso (QE) yazılımı kullanılmıştır. Elektronik bant hesaplamaları 0-200 kBar basınç aralığında SbSeI'nın direkt/dolaylı yasak enerji bant aralığının olduğunu göstermiştir.
Anahtar Kelimeler: SbSeI, Basınç, Elektronik özellikler, Quantum Espresso.

I. INTRODUCTION

If the properties of materials are known, the most suitable material can be selected in terms of cost and performance. Therefore, knowing the properties of materials is important in material science and technology. Peng *et al.* (2018) reported that bulk *V-VI-VII* semiconductors (*V*-family: As, Bi, Sb, *VI*-family: O, S, Se, Te, *VII* family: Br, Cl, F, I) are earth abundant materials [1 - 3] One of the most studied compounds of this family is SbSI [4 – 8]. SbSeI is a member of this group. It has been studied extensively recently [9 - 11]. The synthesis of these materials by exfoliation, hydrothermal method, and sonochemical method are can be experimentally feasible. Antimony selenoiodide (SbSeI) has an orthorhombic structure (space group number: $Pna2_1$) [1].

SbSeI was produced from mixture of antimony (Sb), selenium (Se) and iodine (I) elements [11]. Dubey *et al.* (2014), reported that Nitsche and Merz [12] have synthesized materials like SbSI, SbSBr, SbSeBr, SbSeI, SbTeI, BiSCl, BiSBr, BiSI, BiSeCl, and BiSeBr. They studied their photoconducting properties [8]. Many studies have been carried out on the electrical conductivity [13], electronic, thermoelectric [11], microelectronic, and optoelectronic [1] properties, reflectivity and vibrational spectrum [18] of SbSeI. SbSel's single crystals were grown using the vapor phase technique and the reverse current - voltage (I –V) characteristics of the system were analyzed in the 273 to 363 K temperature range [10]. The structural, elastic, electronic [14] lattice dynamical and thermodynamic [15] properties of SbSeI investigated in the ambient pressure. Nowak *et al.* (2018), the optical parameters of mats of polymeric, polyacrylonitrite nanofibers containing ferroelectric and semiconducting SbSeI were investigated [16]. Mistewicz *et al*. (2019) presented a simple, scalable and inexpensive pyroelectric nanogenerator production method based on SbSeI [17].

Wibowo *et al.* [20] investigated the detection potential of X-rays and γ-rays of the SbSeI compound. The result of the research is showed that among the promising semiconductor materials for high performance X-rays and γ-rays detection of SbSeI [14]. This semiconductor has an indirect band gap value of 2 eV [14, 11, 20]. With a non-linear dielectric properties and strong piezoelectric effect under different phase transitions, this family can be used as a memory element, as well as technologically low pressure sensors can be easily adapted for use in microwaves and piezoelectric devices. [14, 21]. These compounds are technologically important in terms of their physical properties as well as linear and electro optic, piezoelectric, dielectric properties, etc. [22].

Using *ab initio* methods, it is possible to calculate many properties of the material (structural, optical, dynamic and thermodynamic, etc.) with great precision [23]. For electronic and technological applications, it is very

Corresponding Author: Tahsin ÖZER, Tel: +90 328 827 10 00, e-posta: tahsinozer@osmaniye.edu.tr
Submitted: 09.04.2020, **Revised:** 02.09.2020, **Accepted:** 04.10.2020

important to investigate the electronic band structure of the material. The aim of this study is to investigate the structural and electronic properties of the SbSeI crystal at different pressure values up to 200 kBar hydrostatic pressure using QE [24] software. We could not find a study that examined the structural and electronic components of the SbSeI compound under high pressure in the literature examine. For this reason, SbSeI compound was examined for the first time under high pressure with this study.

II. MATERIALS AND METHODS

SbSeI compound has an orthorhombic structure with the Pna2$_1$- C_{2v}^9 (no:33) space group. As shown in Figure 1, it has 12 atoms (4 atoms for Sb, 4 atoms for Se, and 4 atoms for I) per primitive unit cell. All atoms are in the 4c Wyckoff position [25]. The shape of the SbSeI crystal produced by the XCrySDen software [26] using the structural parameters obtained at ambient pressure is shown in Figure 1. The structure of SbSeI compounds consists of chains of atoms along the polar c-axis. It was started to calculations with the structural parameters given in Table 1.

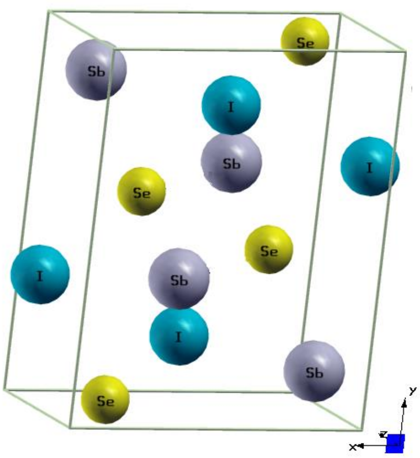

(a)

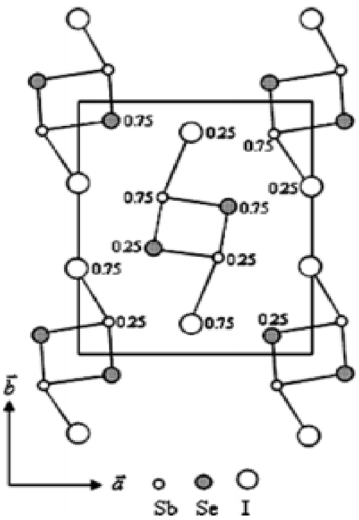

(b)

Figure 1. Illustration (a), schematic projection [28] (b) of the SbSeI crystal.

The structure and electronic properties of SbSeI compound has been studied using DFT as implemented in QE code [24]. The PAW type pseudopotential obtained from the QE website (https://www.quantum-espresso.org/) was used. For this crystal the Monkhorst-Pack k-point mesh [29] $4 \times 4 \times 10$ and plane wave cutoff energy 130 Ry were applied. These k-point mesh and plane wave cutoff are optimized values. The exchange-correction functional is treated within local density approximation (LDA). SbSeI compound is calculated using the convergence threshold on forces (10^{-3} in a.u.) and total energy (10^{-4} in a.u.) for ionic minimization and convergence threshold for selfconsistency (10^{-6}). The 5s^2 p^3 of Sb, 4s^2 p^3 of Se, and 5s^2 p^5 of I orbitals were treated as the valence states. The first Brillouin regions in orthorhombic structure are given in Figure 2. The path used to calculate the band structure is Γ - X - S - Y - Γ - Z - U - R - T - Z - Y - T - U - X - S - R [30].

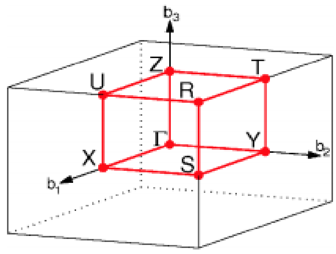

Figure 2. The first Brillouin zone of orthorhombic lattice.

III. RESULTS

In the first stage of our electronic structure calculation, geometric optimization was performed using experimental structural parameters. The optimized values of the structural parameters obtained at ambient pressure (0 kBar) are compared with the literature data in Table 1. It is seen from the table that the calculated lattice parameters agree with the experimental and theoretical results.

Table 1. The structural parameters unit cell of the SbSeI.

	Lattice parameters (Å)			Atomic positions			
Ref.	*a*	*b*	*c*	Atom	*x*	*y*	*z*
This work	8.476	10.211	4.061	Sb	0.126	0.130	0.250
				Se	0.830	0.050	0.250
				I	0.517	0.829	0.250
Exp. [19]	8.698	10.412	4.127				
Exp. [31]	8.686	10.393	4.145				
Theo.[22]	8.474	10.249	4.064	Sb	0.126	0.130	0.250
				Se	0.830	0.050	0.250
				I	0.518	0.829	0.243
Ref [27,28]	8.650	10.380	4.120	Sb	0.118	0.130	0.250
				Se	0.835	0.060	0.250
				I	0.515	0.825	0.250
Ref [25]	8.600	10.300	4.100				

The change of SbSeI crystalline lattice constant, volume and density with pressure is given in Figure 3 by visualizing with MATLAB [32] software. As can be seen from the figure, the lattice constants (*a*, *b* and *c*) and volume decreased with pressure, whereas the density increased. This situation was expected. It is seen from the Figure 3 that *b* is more sensitive to pressure than *a* and *c* which of the lattice constants of SbSeI crystal.

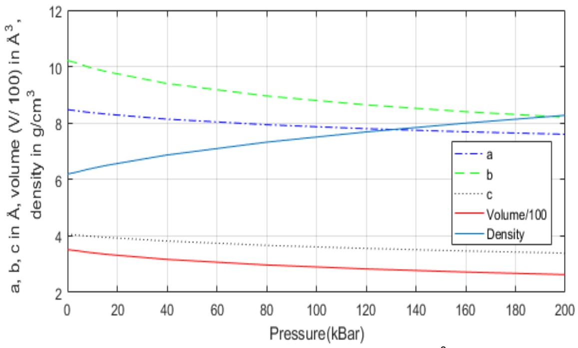

Figure 3. Lattice parameters (*a*, *b*, *c* in Å), volume (V/ 100 in Å^3), and density (g/cm^3) for SbSeI compound as a function of the pressure.

It is a known fact that the structures undergo a phase transition under the influence of temperature or pressure and that the properties of the materials may also change with this phase change. The SbSeI crystal has two phases: (*T* <410 K) antiferroelectric and (*T*> 410 K) paraelectric phase [33].

The derivative of Gibbs free energy with respect to the pressure at constant temperature is equal to volume. In the pressure-based 1st order phase transition, the volume of the unit cell changes suddenly as it passes from one phase to the next. In order to see whether there is a phase transition with the effect of pressure, the pressure-volume graph given in Figure 4 has been drawn. Since the pressure-volume curve given in Figure 4 does not show a discontinuity, it can be said that there is no first order phase transition for SbSeI at the investigated pressure values.

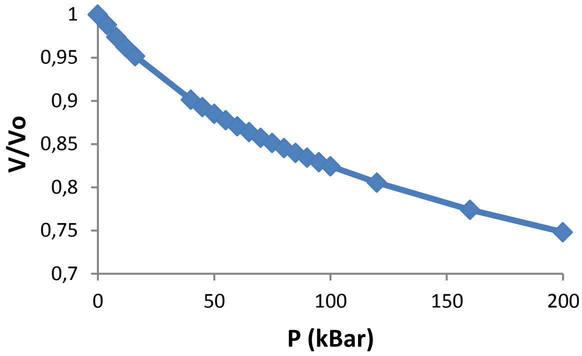

Figure 4. Pressure-volume change curve of SbSeI compound.

Electronic structure analysis plays an important role in analyzing the physical properties of SbSeI crystal from a microscopic perspective [14]. Structural parameters obtained by geometric optimization were used in electronic structure analysis. The high symmetry points of the first Brillouin zone were showed in Figure 5. Zero energy level (Ef) was chosen as the Fermi energy. This energy level was shown on the graph as a horizontal line. It is seen that electronic structures are similar in different pressures (Figure 5). Therefore, in Figure 5, electronic band structure is given only for 0, 80 and 200 kBar pressure values.

(a)

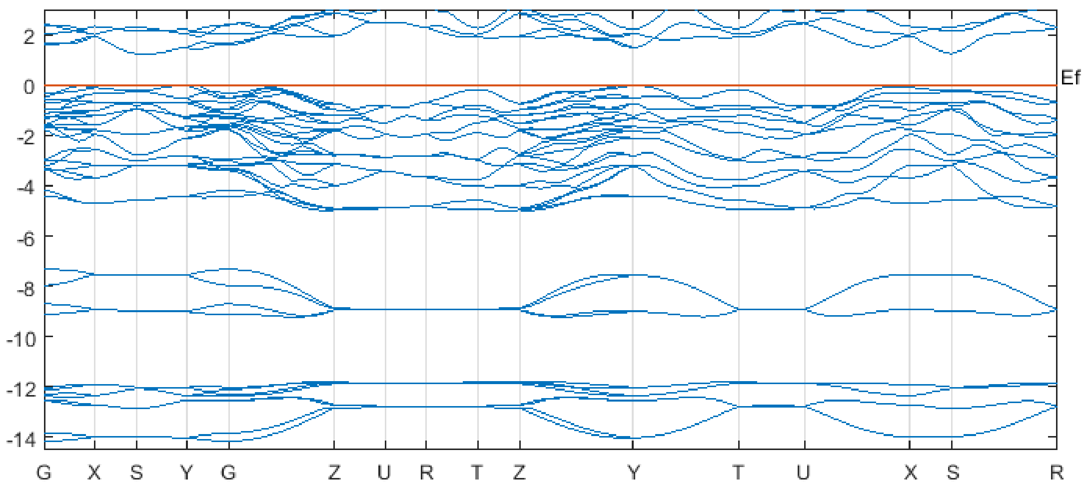

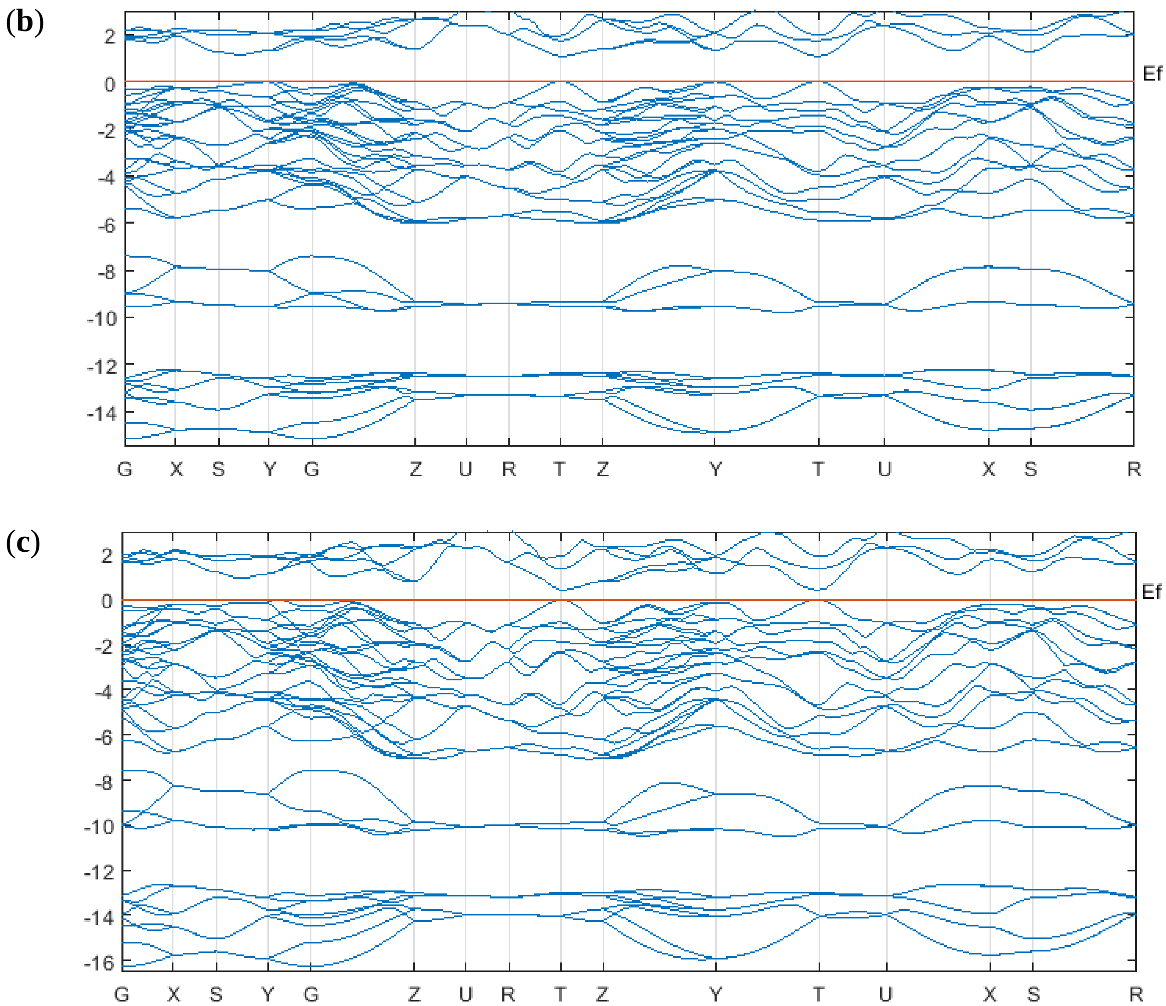

Figure 5. The electronic band structure of SbSeI, (a) 0 kBar, (b) 80 kBar, (c) 200 kBar.

The forbidden band gap of the material occurs between the maximum of the valence band and the minimum of the conductivity band. The material has an indirect band gap occur when the maximum of the valence band and the minimum of the conductivity band correspond to different point. The change of the upper level of the valence band and the lower level of the transmission band with pressure is given in Figure 6. Maximum points of valence band and minimum points of transmission band are marked with "*".

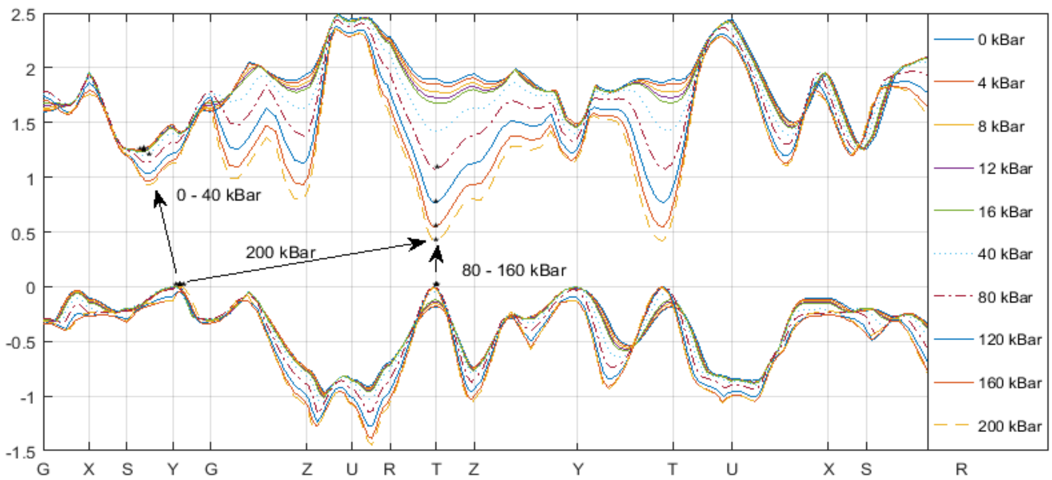

Figure 6. The change of the upper level of the valence band and the lower level of the transmission band with pressure.

As seen in Figure 6, SbSeI has indirect band gap (*Eg*) and direct band gap (*Eg*) in the 0-200 kBar. It is seen that the value of *Eg* decreases with increasing pressure value. The calculated band gap values were compared with the existing experimental and theoretical results available from the literature in Table 2. Ambient pressure was shown in the table as 0 kBar.

Table 2. Band gaps (*Eg*) for SbSeI.

		Band gaps (*Eg*, in eV)	
Pressure (kBar)	This work	Experimental	Other calculated values
0	1.27	1.61 [34], 1.63 [35], 1.70 [36]	1.256 [14], 1.65 [28], 1.33 [1]
4	1.28		
8	1.26		
12	1.26		
16	1.26		
40	1.22		
80	1.07		
120	0.77		
160	0.54		
200	0.43		

In literature review, only ambient pressure studies were found, and no other pressure values were found. Therefore, the data found in other pressure values could not be compared. It is seen that the value found in the ambient pressure is consistent with the value calculated in other theoretical studies (Table 2). The calculated E_g value is smaller than the experimental data. This was expected by the nature of the calculation. Since the band gap values calculated for 0 - 80 kBar pressure values correspond to the visible region (1-3 eV), the SbSeI crystal can be used in applications as a visible light sensor.

The calculated total density of states (TDOS) and partial density of states (PDOS) for SbSeI is shown in Figure 7, to see the contribution of the orbitals to the energy bands. This compound has three valence bands. The lower valence bands were found to be in the range of approximately −17 and −13 eV. It is seen that the greatest contribution to this band comes from the valence s orbitals of Se and I atoms. There is also little contribution from the valence s and p orbitals of the Sb atom. The middle valence bands were found to be in the range of approximately −11 and −6 eV. This band contains predominantly valence s orbitals of the Sb atom. The upper valence bands (in the range of approximately −6 and 0 eV) result from the hybridization of the valence p orbitals of the atoms Sb, Se and I. This hybridization indicates the presence of covalent bond in the compound. Since there is a value in the ambient pressure (Fig. 7 (k)) in the literature, only this pressure value can be compared. It was found that the shape obtained with this study is consistent with the literature data but there is little difference in energy value. This difference is due to the difference used software. It has been observed that density of state valence s orbital (about -8 and -6 eV range), and the p orbital (about -5 and -3 eV range) of Sb atom and p orbital (about -6 and -4 eV range) of the I atom varies in the between 80-200 kBar pressure values.

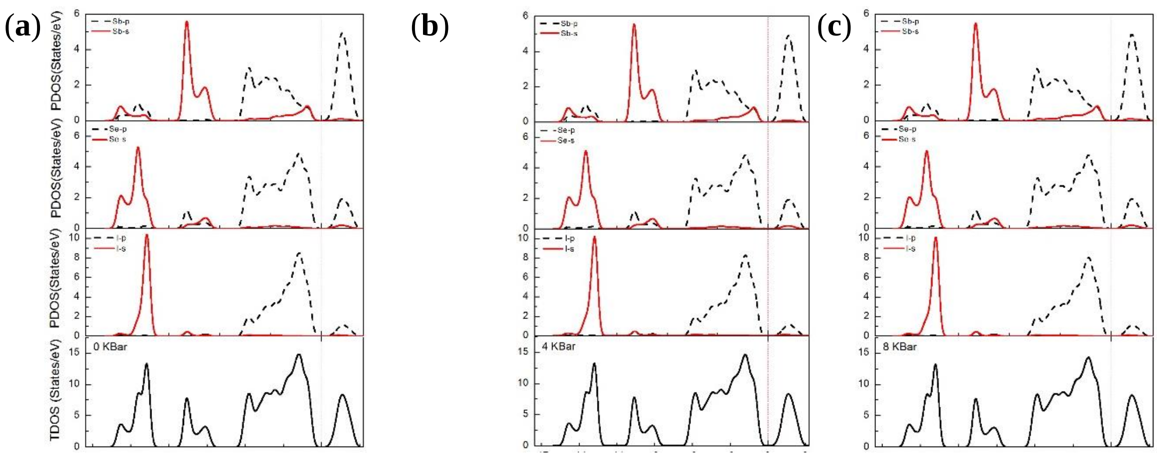

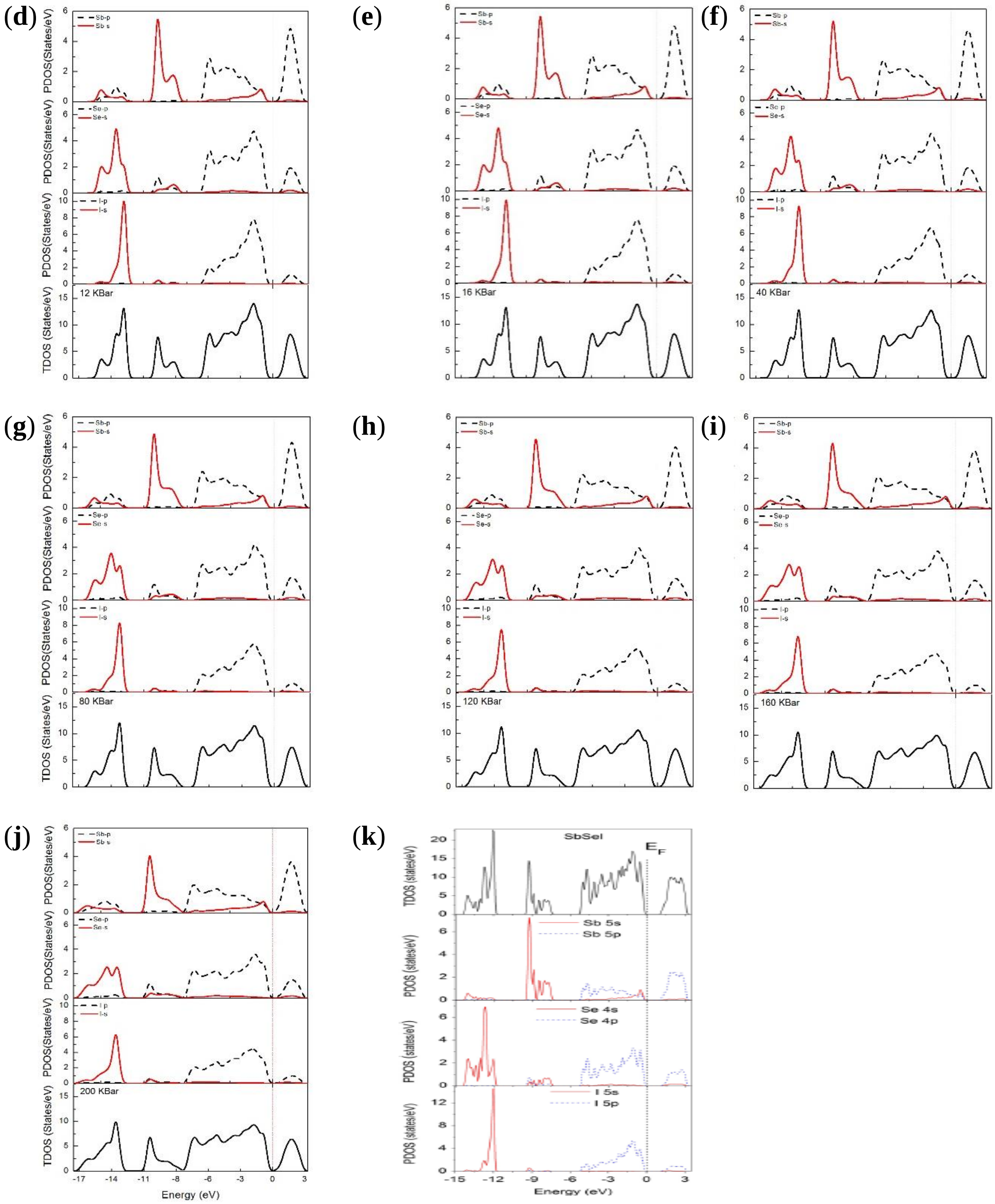

Figure 7. The PDOS and TDOS of SbSeI, (a) 0 KBar, (b) 4 KBar, (c) 8 KBar, (d) 12 KBar, (e) 16 KBar, (f) 40 KBar, (g) 80 KBar, (h) 120 KBar, (i) 160 KBar, (j) 200 KBar, (k) 0 KBar[14]

To describe the structure of the bond between atoms, the two-dimensional charge density distributions in the plane (1 1 1) were generated using the VESTA [37] software. The structure of the chemical bond manages the electron charge density distribution of internal atomic bonds. The figures are given in Figure 8.

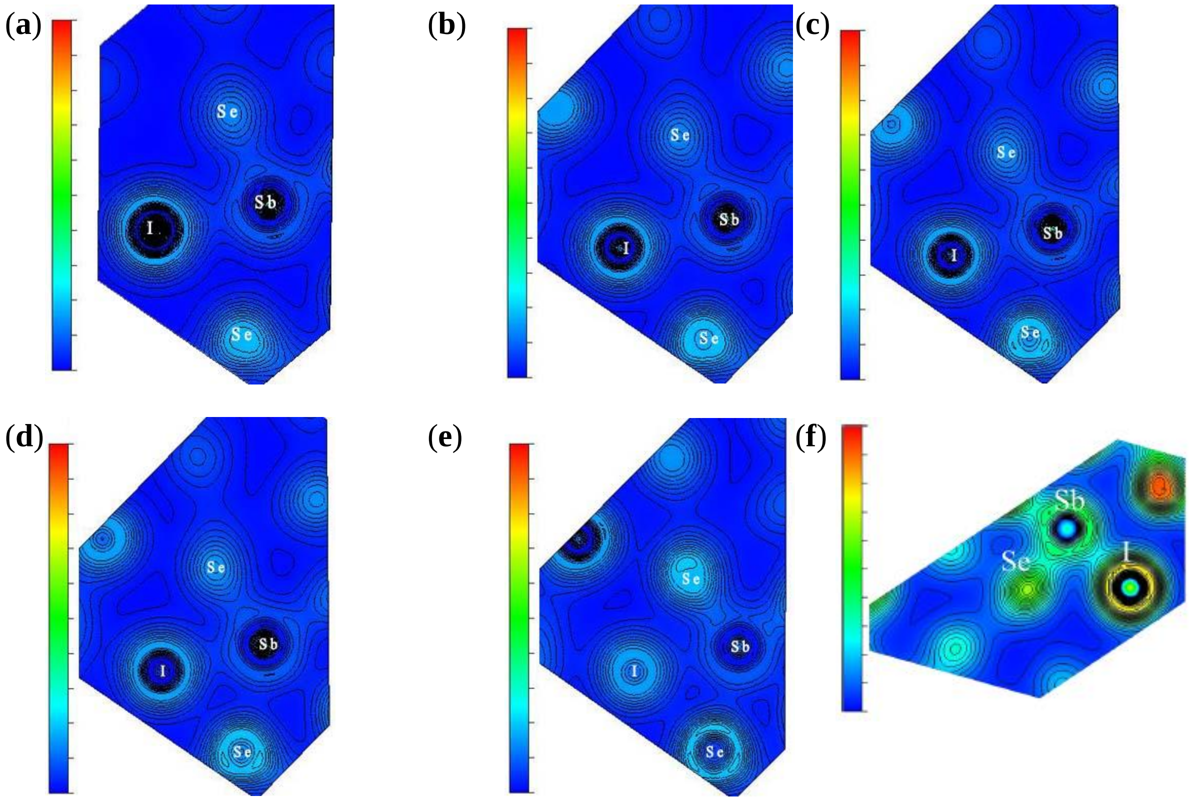

Figure 8. Calculated valence charge density distribution of SbSeI, in the (1 1 1) plane, (a) 0 kBar, (b) 40 kBar, (c) 80 kBar, (d) 120 kBar, (e) 200 kBar, (f) 0 kBar in the (−1 −1 −1) plane. [14] .

The electro negativity values of elements in the SbSeI compound are 1.9 (Sb), 2.4 (Se) and 2.5 (I) [38, 39]. As can be seen from Figure 6, the maximum charge density around the atom I is greater than Sb and Se. This is because the atom I is more electronegative than Sb and Se. Sharing the charge between atoms is important. Because it shows that the bond between atoms is of ionic or covalent character. The spherical charge distribution around the atom I shows that the bond between Sb and I has predominantly ionic character. The presence of hump in the charge density distribution of the Sb and Se atoms indicates that the bond between these atoms is covalent and partly ionic. Physically, after electrons were transferred to the I ion, the Sb and I move away, and a covalent bond was formed. This composite bonding property is called "ionic covalent bond" [14]. The qualitative properties of the load intensities for the SbSeI compound for 0-200 kBar pressure values are very similar. Therefore, visuals are given for 0, 40, 80, 120 and 200 kBar pressure values. This similarity shows that the nature of the bonding between atoms does not change with increasing pressure value.

The percentage of an ionic bond between elements A and B can be determined by the following equation [38].

$$\%\, ionic\ bond\ percentage = \left\{1 - \exp\left[-\frac{(X_A - X_B)^2}{4}\right]\right\} \times 100 \quad (1)$$

Here X_A and X_B are the electronegative values of the related elements. In the periodic table, the electronegativity values of Sb, Se and I are 1.9, 2.4 and 2.5 [38], respectively. The ionic bond percentage values of Sb-I and Sb-Se bonds calculated for the SbSeI structure are 8.61% and 6.06%, respectively. This result confirms the judgment reached above. Accordingly, Sb-Se and Sb-I bonds are weak ionic bonds and strong covalent.

IV. CONCLUSIONS

The aim of this study is to investigate the effect of pressure on the electronic structure of the SbSeI compound. For this purpose, structural optimization of SbSeI compound was performed for 0-200 kBar pressure values. Electronic band structure, TDOS, PDOS and valence charge distributions of SbSeI compound were analyzed using optimized structural parameters. As a result of the analysis, it was seen that the valence charge distribution did not change with pressure, and there was some change in the electronic band and DOS structure after 80 kBar pressure value. In SbSeI crystals, the Sb-Se bond is more covalent than the Sb-I bond. Since the band gap values of SbSeI crystals are in the visible region, they are an important parameter for wide application areas of semiconductor systems.

ACKNOWLEDGMENTS

This work was supported by OKÜBAP (Scientific Research Projects Unit of Osmaniye Korkut Ata University) with the project number OKÜBAP-2018-PT2-001.

We many thank Prof. Dr. Süleyman Çabuk from Çukurova University Faculty of Arts and Sciences for his suggestions and useful criticism.

ORCID

Tahsin Özer http://orcid.org/0000-0003-0344-7118

REFERENCES

[1] Peng, B., Xu, K., Zhang, H., Ning, Z., Shao, H., Ni, G., Li, J., Zhu, Y., Zhu, H., Soukoulis, C.M., (2018). 1D SbSeI, SbSI, and SbSBr With High Stability and Novel Properties for Microelectronic, Optoelectronic, and Thermoelectric Applications. *Adv. Theory Simul.*, 1, 1700005, DOI: 10.1002/adts.201700005

[2] Demartin, F., Gramaccioli, C.M., Campostrini, I., (2015). *Am. Mineral*. 94, 1045.

[3] Demartin, F., Gramaccioli, C.M., Campostrini, I., (2016). *Mineral. Mag.* 74, 141.

[4] Starczewska, A., Nowak, M., Szperlich, P., Toron, B., Mistewicz, K., Stróz, D., Szala, J., (2012). Influence of humidity on impedance of SbSI gel. *Sensors and Actuators A*, 183, 34–42. DOI: 10.1016/j.sna.2012.06.009

[5] Grigas, J., Kajokas, A., Audzijonis, A., Zigas, L., (2001). Peculiarities and properties of SbSI electroceramics. *Journal of the European Ceramic Society*, 21, 337–1340.

[6] Cho, I., Min, B.K., Joo, S.W., Sohn, Y., (2012). One-dimensional single crystalline antimony sulfur iodide, SbSI. *Materials Letters*, 86, 132–135. DOI: 10.1016/j.matlet.2012.07.050

[7] Audzijonis, A., Zaltauskas, R., Zigas, L., Vinokurova, I.V., Farberovich, O.V., Pauliukas, A., Kvedaravicius, A., (2006). Variation of the energy gap of the SbSI crystals at ferroelectric phase transition. *Physica B*, 371, 68–73. DOI: 10.1016/j.physb.2005.09.039

[8] Dubey, H.K., Deshmukh, L.P., Kshirsagar, D.E., Sharon, M., Sharon, M., (2014). Synthesis and Study of Electrical Properties of SbTeI. *Hindawi Publishing Corporation Advances in Physical Chemistry*, Article ID 965350, 6 pages. DOI:10.1155/2014/965350

[9] Audzijonis, A., Zigas, L., Siroic, J., Pauliukas, A., Zaltauskas, R., Cerskus, A., Narusis, J., (2006). Investigation of the electronic structure of the SbSeI cluster. *Phys. Stat. Solidi B*, 243, 610-617. DOI: 10.1002/pssb.200541376

[10] Audzijonis, R., Sereika, R., Lapeika, V., Zaltauskas, R., (2007). Current mechanism in SbSeI crystals based on phonon-assisted tunnelling emission. *Phys. Stat. Solidi B*, 244, 3260-3264. DOI: 10.1002/pssb.200642438

[11] Khan, W., Hussain, S., Minar, J., Azam, S., (2017). Electronic and thermoelectric properties of ternary chalcohalide semiconductors: First principles study. *Journal of electronic materials*, DOI:10.1007/s11664-017-5884-z

[12] Nitsche R., and Merz, W.J., (1960). Photoconduction in ternary V-VI-VII compounds. *Journal of Physics and Chemistry of Solids*, 13, 154–155. DOI: 10.1016/0022-3697(60)90136-0

[13] Nejezchleb K., and Horak, J., (1968). Preparation and photoelectric properties of antimony selenium iodide. *Czech. J. Phys. B*, 18, 138 -142.

[14] Ozer, T., Cabuk, S., (2018). First-principles study of the structural, elastic and electronic properties of SbXI (X=S, Se, Te) crystals. *Journal of Molecular Modeling*, 24:66. DOI:10.1007/s00894-018-3608-9

[15] Ozer, T., Cabuk, S., (2018). Ab initio study of the lattice dynamical and thermodynamic properties of SbXI (X= S, Se, Te) compounds. *Computational Condensed Matter*, 16, e00320. DOI:10.1016/j.cocom.2018.e00320

[16] Nowak, M., Kępińska, M., Tański, T., Matysiak, W., Szperlich, P., Stróżc, D., (2018). Optical properties of nanocomposite fibrous polymer mats containing SbSeI nanowires. *Optical Materials*, 84, 383-388. DOI: 10.1016/j.optmat.2018.07.012

[17] Mistewicz, K., Jesionek, M., Nowak, M., Kozioł, M., (2019). SbSeI pyroelectric nanogenerator for a low temperature waste heat recovery. *Nano Energy*, 64, 103906. DOI:10.1016/j.nanoen.2019.103906

[18] Audzijonis, A., Klingshirn, C., Žigas, L., Goppert, M., Pauliukas, A., Žaltauskas, R., Čerškus, A. Kvedaravičius, A., (2007). Investigation of the vibrational spectrum of SbSeI crystals in harmonic and in the anharmonic approximations. *Phys B: Condens Matter*, 393, 110–118. DOI: 10.1016/j.physb.2006.12.053

[19] Wibowo, A.C., Mallakas, C.D., Liu, Z., Peters, J.A., Sebastian, M., Chung, D.Y., Wessels, B.W., Kanatzidis, M.G., (2013). Photoconductivity in the chalcohalide semiconductor, SbSeI: a new candidate for hard radiation detection. *Inorg Chem*, 52, 7045–7050. DOI: 10.1021/ic401086r

[20] Pikka, T.A., and Fridkin, V.M., (1968). Fiz. Tverd. Tela. 10, 3378.

[21] Sobolev, V. Val., Pesterev, E.V., Sobolev, V. V., (2004). Absorption Spectra of SbSeI and BiSeI Crystals. *Inorganic Materials*, 40, 16–19.

[22] Ozer, T., (2016). Investigation of Structural, Dynamic and Thermodynamic Properties of SbXI (X = S, Se, Te) Compounds with ab Initio Method, PhD thesis, *Çukurova University Institute of Natural and Applied Sciences Department of Physics*, 148 Pages, Adana, (Turkish).

[23] Bilge, M., Kart, S.Ö., Kart, H.H., Çağın, T., (2008). B3-B1 phase transition and pressure dependence of elastic properties of ZnS. *Materials Chemistry and Physics*, 111, 559-564. DOI: 10.1016/j.matchemphys.2008.05.012

[24] Available from: http://www.quantum-espresso.org

[25] Shiozaki, Y., Nakamura, E., Mitsu, T.(eds), (2002). "Ferroelektrics and related substances",

Londalt-Börnstein. Numerical data and functional relationships in science and technology, 36, II data: 14 SbSI family.
[26] Available from: http://www.xcrysden.org/
[27] Wyckoff, R. W. G., (1980). Crystal Structures, 1 (Interscience, New York, 1980), p. 385.
[28] Akkus, H., Kazempour, A., Akbarzadeh, H., Mamedov, A.M., (2007). Bant structure and optical properties of SbSeI:density-functional calculation. *Phys. Stat. Sol.* (b), 244, 3673–3683.
[29] Monkhorst, J.H., Pack, J.D., (1976). Special points for Brillouin-zone integrations. *Phys Rev B*, 13, 5188–5192
[30] Setyawan, W., Curtarolo, S., (2010). High-throughput electronic band structure calculations: Challenges and tools. *Computational Materials Science*, 49, 299-312. DOI:10.1016/j.commatsci.2010.05.010
[31] Voutsas, G.P., Rentzeperis, P.J., (1982). The crystal structure of antimony selenoiodide, SbSeI. *Crystalline Materials*, 161, 111-118. DOI: 10.1524/zkri.1982.161.14.111
[32] Available from: https://www.mathworks.com
[33] Audzijonis, A., Sereika, R., Žaltauskas, R., (2008). Antiferroelectric phase transition in SbSI and SbSeI crystals. *Solid State Communications*, 147, 88-89. DOI:10.1016/j.ssc.2008.05.008
[34] Jesionek, M., Nowak, M., Szperlich, P., Stróż, D., Szala, J., Jesionek, K., Rzychoń, T., (2012). Sonochemical growth of antimony selenoiodide in multiwalled carbon nanotube. *Ultrasonics Sonochemistry*, 19, 179-185. DOI: 10.1016/j.ultsonch.2011.06.006
[35] Nowak, M., Kauch, B., Szperlich, P., Jesionek, M., Kępińska, M., Bober, L., Szala, J., Moskal, G., Rzychoń, T., Stróż, D., (2009). Sonochemical preparation of SbSeI gel. *Ultrasonics Sonochemistry*, 16, 546-551. DOI: 10.1016/j.ultsonch.2009.01.003
[36] Madelung, O., (2004). Semiconductors: data handbook. In:Madelung O (eds) V-I-VI I compounds, *Springer*, Berlin, pp 664–673.
[37] Momma, K., Izumi, F., (2011). VESTA 3 for three-dimensional visualization of crystal, volumetric and morphology data. *J Appl Crystallogr*, 44:1272–1276.
[38] Callister, WD., Rethwisch, DG., (2011). Materials science and engineering. 8th edn, *Wiley*, New York, pp 26–36.
[39] Lefebvre, I., Lannoo, M., Allan,G., (1987). Electronic properties of antimony chalcogenides. *Phys Rev Lett*, 59:2471–2474.